

In Vivo Study of Anticancer Agent Temozolomide by $^1\text{H}/^{13}\text{C}$ MRI/MRS

Y. Kato¹, B. Okollie¹, Z. M. Bhujwalla¹, D. Artemov¹

¹Radiology Department, NMR Research, The Johns Hopkins University School of Medicine, Baltimore, MD, United States

Abstract

One of the reasons for anticancer drugs failure is thought to be physiologic drug resistance or insufficient drug delivery to the tumor due to an inadequate tumor vascularization and/or anti-vascular effects of the chemotherapy. We studied intratumoral distribution of ^{13}C -labeled anticancer agent temozolomide (^{13}C]TMZ) in mouse breast cancer models using *in vivo* MR spectroscopic imaging (CSI). Inverse ^{13}C detection with heteronuclear multiple quantum coherence (HMQC) provided an optimum sensitivity of detection. Three-dimensional maps of drug distribution (2mm isotropic resolution) were obtained following intraperitoneal administration of ^{13}C]TMZ. The status of the tumor blood supply was assessed by gadolinium enhanced dynamic MRI.

Introduction

Physiological drug resistance has been recognized as one of the major problems for anticancer chemotherapy (1). The antiangiogenic effects of traditional chemotherapy may inflict additional damage to already inadequate tumor vasculature. Together with multi-drug resistance type mechanisms this leads to a significantly reduced exposure of cancer cells to the drug. Therefore *in vivo* determination of intratumoral drug distributions is an important problem in cancer chemotherapy. Temozolomide, a relatively novel cytotoxic anticancer agent, can be labeled with ^{13}C isotope and its resonance can be detected in tumors using *in vivo* ^{13}C MR spectroscopy (MRS) (2). In this study we attempted to detect the spatial distribution of the drug in the tumor, which required significant enhancement of the sensitivity of detection. We therefore implemented a 3D CSI variant of the HMQC pulse sequence with broad-band ^{13}C decoupling. The sequence provided an efficient suppression of water and significant attenuation of the lipid peak thus enabling sensitive detection of the ^{13}C]TMZ proton signal. Efficiency of the drug delivery depends upon the status of tumor vasculature including perfusion and vascular permeability. These parameters were independently measured using GdDTPA enhanced dynamic 3D MRI.

Methods

Human breast carcinoma MCF-7 cells were orthotopically implanted into severe combined immunodeficient (SCID) mice (female, approx. 18 g). Phantom experiments were performed with ^{13}C]TMZ (20 mg/ml, 99% ^{13}C at the methyl position, Cambridge Isotope Laboratories, Inc., MA, U.S.A.) or 90% methanol. Omega-400 9.4T spectrometer (GE/Bruker) equipped with mini-imaging gradients (130 G/cm) and a home-built probe with a double-tuned $^{13}\text{C}/^1\text{H}$ RF coil and narrow-path ^1H and ^{13}C RF filters was used in all studies. A phantom was used for comparison of direct ^{13}C and indirect ^1H detections schemes. Anesthetized mice were immobilized in the probe and maintained under gas anesthesia (Isoflurane 0.5%, 1 l/min), body temperature was stabilized by a hot air flowing through the probe, respiration rate was controlled with a soft pad attached to the pressure transducer. Twenty mg/ml of ^{13}C]TMZ was infused via an i.p. catheter at a constant rate of 2.0 ml/h for 10 min followed by slow-rate infusion of 1.0 ml/h for the rest of the experiment. 3D HMQC CSI experiment was performed with an 8x8x8 matrix for a 16 mm isotropic field of view. K-space was sampled with an optimized averaging scheme and the effective number of scans was varied from 4 at the edges of the K-space to 48 for the central voxels. The total acquisition time was kept below 1 hour. After completing ^{13}C studies, a GdDTPA bolus was administered and 3D isotropic gradient echo imaging (TE/TR = 5/200 ms) was performed before and for 10min after the contrast. All animal experiments were conducted according to the institutional guidelines.

Results

Figure 1 compares decoupled spectra of ^{13}C]TMZ using direct (NOE) ^{13}C - and indirect ^1H -MRS. Signal-to-noise ratio (SNR) of indirect ^1H -MRS was about 2.3-fold larger than that of the former for similar acquisition time and optimized processing. 3D-image of 90% methanol phantom reconstructed from 3D CSI maps is shown in Fig.2. Highly uniform signals were detected in this image. Figure 3 shows 3D $^1\text{H}\{^{13}\text{C}\}$ image after ^{13}C]TMZ administration reconstructed by integration of the drug peak in 3D CSI maps. This image indicated nonuniform drug distribution within the tumor. Corresponding contrast uptake maps are shown in Fig. 4. GdDTPA uptake was more pronounced in the peripheral regions of the tumor.

Discussion

HMQC pulse sequence used in this study provided a significantly enhanced sensitivity for detection of the $^{13}\text{CH}_3$ resonance of ^{13}C]TMZ. The method enabled acquisition of *in vivo* maps of the drug in the tumor with a spatial resolution of about 10 mm³. Nonuniform distribution of the drug and correspondingly heterogeneous distribution of the contrast uptake was detected in the tumors. The method makes it feasible to study the delivery pattern of the drug and co-registered contrast uptake in the course of chemotherapy. This allows us to detect emerging physiological drug resistance and modulation in the tumor vascular supply caused by cytotoxic chemotherapy. To include the MDR axis into the consideration, further experiments with fluorescent MDR ligands as well as immunohistological studies of MDR P-glycoprotein expression are in progress in our laboratory.

Conclusion The HMQC pulse sequence used in this study was very effective for the detection of ^{13}C -TMZ by indirect ^1H -MRS. In addition, it was conceivable that the insufficient drug distribution to the tumor tissue was responsible for physiological drug resistance. Future TMZ chemotherapy and MDR detection study might give us invaluable information on physiological drug resistance.

Acknowledgements This work was supported by NIH grant RO1 CA097310.

References: 1. Teicher, BA et al., Science, 247, 1457-61 (1990); 2. Artemov, D et al., Magn. Reson. Med., 34, 338-42 (1995).

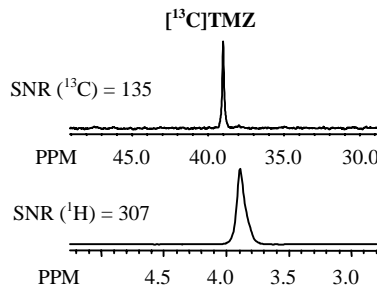


Figure 1 Comparison of direct vs. indirect ^{13}C MRS.

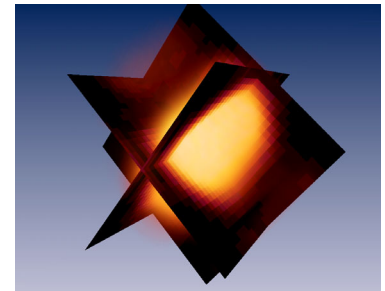


Figure 2 3D CSI scan of CH_3OH phantom (17 min.)

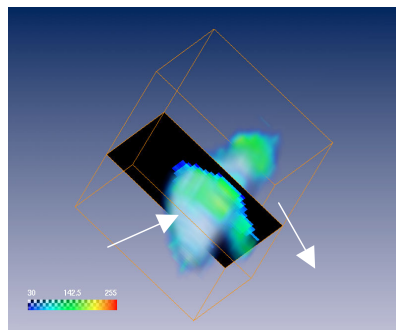


Figure 3 Intratumoral Distribution of ^{13}C]TMZ.
Grayscale image: water map, Color image: drug map.

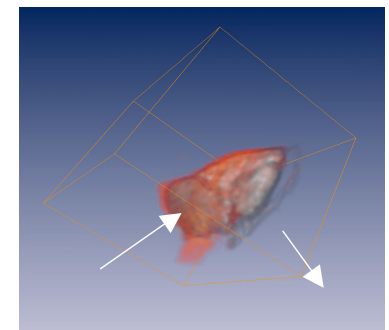


Figure 4 T1 Weighted MRI of GdDTPA uptake
Grayscale image: precontrast map, Red: difference map.